X-602-77-39

PREPRINT

TMX 71279

# TOTAL BORN APPROXIMATION CROSS SECTIONS FOR SINGLE ELECTION LOSS BY ATOMS AND IONS COLLIDING WITH ATOMS



D. W. RULE


FEBRUARY 1977

GSFC

GODDARD SPACE FLIGHT CENTER

GREENBELT, MARYLAND

# TOTAL BORN APPROXIMATION CROSS SECTIONS FOR SINGLE ELECTRON LOSS BY ATOMS AND IONS COLLIDING WITH ATOMS

D. W. Rule*

NASA/Goddard Space Flight Center
Greenbelt, Maryland 20771

*National Research Council Research Associate

## ABSTRACT

We have applied the first Born approximation (FBA) to the calculation of single electron loss cross sections for various ions and atoms containing from one to seven electrons. Screened hydrogenic wave functions were used for the states of the electron ejected from the projectile and Hartree-Fock elastic and incoherent scattering factors were used to describe the target. The effect of the target atom on the scaling of projectile ionization cross sections with respect to the projectile nuclear charge was explored in the case of hydrogen-like ions. We also have examined scaling of the cross section with respect to the target nuclear charge for electron loss by $Fe^{+25}$ in collision with neutral atoms ranging from H to Fe. These results were compared to those of the binary encounter approximation (BEA) and to the FBA for the case of ionization by completely stripped target ions. We have also calculated electron loss cross sections for the ions $O^{+i}$ (i=3-7) and $N^{+i}$ (i=0-6) in collision with He targets in the energy range of $\sim$0.1 to 100 MeV/nucleon. We found these results to be in excellent agreement with the available data near the peak of the ionization cross section.

## I. Introduction

Cross sections for the ionization of highly charged heavy ions by light neutral atoms are necessary for the calculation of relative abundances of various charge states in low energy cosmic rays. Theoretical values for these cross sections and an assessment of their reliability in the 0.1-100 MeV/nucleon regime are particularly important because of the paucity of experimental values for some of the cases of astrophysical interest. For these reasons we have calculated single electron loss cross sections in the first Born approximation (FBA) for hydrogen-like and helium like ions, as well as for ions with more than two electrons. In our calculations, the ejected electron is described by screened hydrogenic wavefunctions and the neutral target atoms are characterized by Hartree-Fock form factors.

The present application of the FBA to ion-atom collisions follows closely the methods developed extensively by Bates and his co-workers.[1,2] Most of the earlier theoretical work[1-7] using the FBA to calculate ionization processes was applied to hydrogen-like and helium-like systems being ionized by hydrogen and helium atoms. There have also been several FBA calculations [6,8-11] for electron loss by H and He in heavy neutral targets, which treat the target using a closure approximation for the infinite sum over final target states. However, few calculations are available for heavy projectiles with more than two electrons colliding with neutral atoms. As a result, scaled binary encounter approximation (BEA) ionization

cross sections have often been used to calculate relative abundances of the ionic charge states in beams of low energy cosmic rays. Scaled BEA cross sections have the advantages of availability in the literature and ease of calculation; however, to use this approximation, one must argue that the structure of the target atom, usually H or He, is not important in the ionization process. The validity of such an argument is not completely clear in all cases. We have therefore included a comparison of the present FBA results with those from the scaled BEA[12] to help determine the latter method's reliability and accuracy.

We also have examined the scaling properties of the cross sections for hydrogen-like ions with respect to both target and projectile nuclear charges for projectiles ranging from H to $Fe^{+25}$, and for neutral targets ranging from H to Fe. Finally, we have compare: our results for the ionization of $N^{+i}$(i=0-6) and $O^{+i}$(i=3-7) by He with experimental data in the energy range from 0.1 to 10 MeV/nucleon. These comparisons have proved very useful in determining the expected region of validity of the FBA and the BEA in cases necessary for the study of low energy cosmic ray ions, for which no data is available.

## II. Method of Calculation

In our calculations, we assume that the major contribution to the loss of a single electron is direct Coulomb ionization. We then write the total ionization cross section as a sum over partial cross sections for each occupied subshell of the projectile:

$$\sigma(V) = \sum_{n=1}^{N} \sum_{\ell} \sigma_{n,\ell}^{T}(V) , \tag{1}$$

where N is the principle quantum number of the highest occupied shell, and V is the relative velocity of the projectile-target system. Each $\sigma_{n,\ell}^{T}$ can be separated into two parts, one in which the target remains in the ground state, $\sigma_{n,\ell}^{E}$, and one which is the sum over all inelastic target processes, $\sigma_{n,\ell}^{I}$, as

$$\sigma_{n,\ell}^{T}(V) \equiv \sigma_{n,\ell}^{E}(V) + \sigma_{n,\ell}^{I}(V) . \tag{2}$$

After Fourier transforming the potential in the usual expression for the FBA cross section, one obtains for $\sigma_{n,\ell}^{E,I}(V)$ (see, for example refs. 2,4,10):

$$\sigma_{n,\ell}^{E}(V) = 8\pi a_0^2 \left(\frac{Z_T V_0}{V}\right)^2 \int_{q_1}^{q_2} \frac{dq}{q^3} \left|1 - F(q)\right|^2 \left[\int_0^{k_{max}} k^2 dk\, \mathcal{E}_{n,\ell}(k,q)\right]^2, \tag{3}$$

and

$$\sigma_{n,\ell}^{I}(V) = 8\pi a_0^2 \left(\frac{V_0}{V}\right)^2 Z_T \int_{q_1'}^{q_2'} \frac{dq}{q^3} S(q) \int_0^{k'_{max}} k^2 dk\, \mathcal{E}_{n,\ell}(k,q) . \tag{4}$$

In the above expressions we have: $a_0$ the Bohr radius, $v_0 \equiv \alpha c$ the Bohr velocity, $Z_T$ the target nucleus, and $\vec{q} \equiv \vec{K}_f - \vec{K}_i$,

where $\vec{K}_i$ and $\vec{K}_f$ are the initial and final momenta in the center of mass system in $a_o^{-1}$.

The target elastic form factor F(q) is given by

$$F(q) \equiv \sum_i F_{ii}(q) \tag{5}$$

(summed over occupied spin-orbitals), where,

$$F_{ij}(q) \equiv \frac{1}{Z_T} \langle \psi_i(\vec{r}) | e^{i\vec{q}\cdot\vec{r}} | \psi_j(\vec{r}) \rangle_{\vec{r}} , \tag{6}$$

in which $\psi_i(\vec{r})$ is a single particle spin-orbital for a target electron with coordinate $\vec{r}$ measured from the target nucleus. The incoherent scattering form factor, S(q) in (4), is defined by

$$Z_T S(q) \equiv N_T - Z_T^2 \left[ \sum_i |F_{ii}(q)|^2 + \sum_{i \neq j} F_{ij}^*(q) F_{ij}(q) \right], \tag{7}$$

where $N_T$ is the number of target electrons ($N_T = Z_T$ for neutrals).

The function $\varepsilon_{n,\ell}(k,q)$ for the ionized projectile is given by[14]

$$\varepsilon_{n,\ell}(k,q) \equiv \frac{N_{n,\ell}}{2\ell+1} \int d\hat{k} \sum_{m=0}^{\ell} (2-\delta_{m,0}) \left| \langle \vec{k}, Z_P^f | e^{i\vec{q}\cdot\vec{r}} | n\ell m, Z_P^i \rangle \right|^2 , \tag{8}$$

which is just the inelastic form factor for a bound to continuum transition, averaged over m, integrated over the angle $\hat{k}$ of the ionized electron, and multiplied by the number of electrons in the subshell, $N_{n,\ell}$. The wave functions are hydrogenic functions with effective charges $Z_p^i$ for the initial state and $Z_p^f$ for the final state. The states $|\vec{k}, Z_p^f\rangle$ and $|n\ell m, Z_p^i\rangle$ have been constructed to be

orthogonal[14] in order to avoid additional terms in (8) from the interaction of the projectile nucleus with both the target nucleus and the target's electrons, which would otherwise appear when $Z_p^f \neq Z_p^i$. The effective charges can be specified for each pair of quantum numbers $(n,\ell)$.

We note that if $Z_p^f = Z_p^i$, then $\mathcal{E}_{n,\ell}(k,q)$ can be obtained by defining $Q \equiv q/Z_p^i$ and using $\mathcal{E}_{n,\ell}(k,Q)$ evaluated with $Z_p^f = Z_p^i = 1$ in (8) above. The eqs. (3) and (4) can be rewritten in terms of Q. From this it is seen[4] that in terms of the scaled velocity,

$$v \equiv V/(Z_p^i v_0) , \tag{9}$$

we find the following approximate relations for $v>>1$:

$$\sigma_{n,\ell}^E(v) \propto Z_T^2/(Z_p^{i2} v)^2 ; \tag{10}$$

and

$$\sigma_{n,\ell}^I(v) \propto Z_T/(Z_p^{i2} v)^2 . \tag{11}$$

Finally, we discuss the limits of integration appearing in (3) and (4). The momentum q takes on its maximum and minimum values, $q_2$ and $q_1$, when k = 0:

$$q_{2,1} = K_i \pm K_i\left[1-\frac{\mu}{m_e K_i^2}(I_p + \Delta E_T)\right]^{1/2} \tag{12a}$$

$$\approx K_i \pm K_i\left[1-\frac{\mu}{2m_e K_i^2}(I_p + \Delta E_T)\right] , \tag{12b}$$

with $\mu$ being the reduced mass of the projectile-target system, $m_e$ the electron's mass, $I_p$ the ionization potential in Rydbergs for the $(n,\ell)$ subshell of the projectile, and $\Delta E_T$ the change in the target's internal energy. For $q_1$ and $q_2$ in (3) $\Delta E_T \equiv 0$ and we have

$$q_1 \approx \mu I_p / (2 m_e K_i) = I_p / (2 v Z_p^i) \tag{13}$$

and

$$q_2 \approx 2K_i \quad . \tag{14}$$

For $q_1'$ and $q_2'$ in (4), we must use an effective target excitation energy for $\Delta E_T$, since the expression for $\sigma^I_{n,\ell}(V)$ was derived by using closure to sum over all inelastic target states. We have adopted the procedure of Lodge[6] and let

$$\Delta E_T \equiv I_p + k^2 \quad . \tag{15}$$

Alternative choices for $\Delta E_T$ have been studied previously[4]; also, corrections to the closure approximation have been calculated.[15] Using (15) in (12b) we obtain

$$q_1' \approx (I_p + I_T) / (2 v Z_p^i) \tag{16}$$

In the actual calculation we take $q_2, q_2' \to \infty$. The upper limit of the

k integration, $k_{max}$ in (3), is given by

$$k_{max} = \left[ \frac{m_e}{\mu} \left( 2 q K_i - q^2 \right) - I_P \right]^{1/2}, \qquad (17)$$

while (15) gives

$$k'_{max} = \left[ \frac{m_e}{2\mu} \left( 2 q K_i - q^2 \right) - \frac{1}{2} \left( I_P + I_T \right) \right]^{1/2} \qquad (18)$$

for $k'_{max}$ in (4).

## III. Results

In this section we will describe the results of applying the theory outlined in the previous section. In order to carry out the calculations, we have used analytic fits[16] to Hartree-Fock elastic form factors for F(q) in (3). For the incoherent scattering factor defined in (7), we have used those obtained by Cromer.[17] The projectile inelastic form factor in (8) was obtained as in ref. (14), using screened hydrogenic wave functions. For each subshell we have used effective charges $Z_p^i$ calculated by Block and Mendelsohn.[18] Other choices of effective charges[19,20] would alter our results by an amount which is smaller than the error associated with the experimental data in most cases considered here. The ionization potentials for each subshell were obtained from Moore's Tables.[21]

### A. Hydrogen-like Projectiles

Fig. 1 contains the results of calculations for electron loss from $H^0$, $O^{+7}$, and $Fe^{+25}$ in collisions with both He and C targets. To examine scaling with respect to $Z_p$ (see eqs. (10) and (11)) we have plotted $Z^4 \equiv Z_p^4$ times the total cross section in $cm^2$ versus the scaled velocity, v (eq. (9)). The H-He data shown for comparison is from Toburen et. al.[22] and Stier and Barnett[23]. These He results are similar to those obtained by Dmitriev et.al.[3] (see fig. 3b of ref. 3). The carbon target results have been displaced to the right by one decade (upper scale) for clarity. The H-C data[22] was deduced from data for H on $H_2$, $O_2$, $CO_2$, $CH_4$, $C_2H_2$, $C_2H_6$, and $C_4H_{10}$, using the sum rule for the measured cross sections, neglecting molecular effects.

We see that $Z_p$ scaling for projectiles of higher charge is quite good for He targets, but for C targets the scaling is reduced. The scaling for high $Z_p$ can be understood from the fact that $q_1$ and $q_1'$ of eqs. (13) and (16) are proportional to $Z_p^2$. Thus the minimum momentum transfer required for ionization is much larger for high $Z_p$, and the q integration of eqs. (3) and (4) covers a range in which only the tails of $F(q) \ll 1$ and $S(q) \approx 1$ are seen. Thus, for large $Z_p$, scaling is quite good for He, while for C, the influence of F(q) and S(q) extends to large q values, reducing the scaling.

Comparison of the H-He and H-C calculations with experiment indicates that the FBA for heavier targets is inadequate near the peak of the cross section ($v \approx 1$). Similar results have been obtained by others[8,9,11]. Walters[10] has treated this problem in terms of an exact calculation of $\sigma_{1S}^{E}$ for ionization in the static field of the target. The inelastic target contribution $\sigma_{1S}^{I}$ was still calculated in the FBA. His results for H-A agree much better with experiment than do results based on the FBA for $\sigma_{1S}^{E}$, however this method requires considerably more computational effort.

In Fig. 2 we show the results of ionization cross sections for $Fe^{+25}$ losing its electron as a result of colliding with H, He, C, and Fe target atoms. The dashed line is the binary encounter approximation (BEA) as tabulated by Hansen,[13] which we have extrapolated beyond the range he has given. The dashed-dot line is the FBA result for protons as targets (FBAP), which scales exactly as $Z_T^2$ for other bare nuclei as targets. The ordinate is $(Z_p^4/Z_T^2)$ times the total ionization cross section, and the abscissa

is v, eq. (9). Thus this set of curves tests the scaling of the total cross section, $\sigma^T$ eq. (2), with respect to the target charge. Actually the $Z_T^2$ scaling is appropriate for $\sigma^E$, while $\sigma^I$ scales as $Z_T$(c.f. eqs. (10), (11)). The BEA and FBAP curves scale exactly as $Z_T^2$, since bare nuclei don't yield a contribution to the total cross section corresponding to $\sigma^I$ for the neutral targets. Although the latter curves are not truly comparable to results for ionization by neutral atoms, we have included them for the reason discussed in Section I. As seen in Fig. 2, for the $Fe^{+25}$ ionizing in H, the BEA is $\sim$ 40% lower than our results for v = 1. At higher energies the discrepancy increases.

We have found that $Z_T^{-2}\ \sigma^E$ and $Z_T^{-1}\ \sigma^I$ obey scaling quite well if scaled separately. We also find that the curve for protons as targets, FBAP, is nearly identical to the elastic target cross section, $\sigma^E$, for neutral hydrogen below v $\approx$ 3; for v = 20, the FBAP result exceeds $\sigma^E$ by $\sim$ 47%. This result is expected, since, for charged targets, the long range Coulomb force gives rise to an $E^{-1}$ log E energy dependence, in contrast to the $E^{-1}$ dependence for neutral targets. The fact that the lighter targets give scaled ionization cross sections which are above the FBAP curve, while the heavier targets give values below the FBAP curve is explained by the fact that $\sigma^I/\sigma^E \propto 1/Z_T$. Thus the relative contribution to $\sigma^T$ from $\sigma^I$, eq. (2), is reduced for heavy neutral targets.

B. Multi-electron projectiles

In Fig. 3 we give the FBA results for total ionization cross sections as a function of energy calculated for several charge states of oxygen being ionized by He. Also shown are BEA cross sections for $He^{+2}$ targets and the data of MacDonald and Martin[24] and Dmitriev et. al.[25,26] No error bars were displayed in ref. 23. However we have estimated the bars from the discussion given there and included them in our figure in order to aid in comparing our results to the BEA and to experiment, as well as to compare the four lowest energy data points of ref. (24) to the higher energy data.

The FBA results (solid curves) were calculated by summing the $\sigma^T_{n,\ell}$'s with respect to n and $\ell$, as in eq. (1), using $Z_p^f = Z_p^i$ (see eq. (8)) in each case. For the lower charge states in which the 2s electrons were involved, we did not recalculate $\sigma^T_{1s}$ with altered screening and ionization potential since $\sigma^T_{1s}$ was only a small contribution to the total cross section as compared to $\sigma^T_{2s}$. The effect of the additional screening by an outer electron can be seen in the case of $O^{+3}$, where there is one electron in a 2p state. For this case we show both the result of the uncorrected sum, $\sigma^T_{1s} + \sigma^T_{2s} + \sigma^T_{2p}$, (solid curve) and of the sum in which $\sigma^T_{2s}$ was recalculated (dash-dot curve) with the additional screening and altered ionization potential coming from the outer 2p electron. We conclude from this that such additional screening is only important for the lower charge states of the ion, in which the 2p subshell begins to fill. For heavier, more highly charged projectiles such as Fe, the effect of additional screening of the inner electrons

by the outer ones should be even less than in the case of oxygen.

In comparing our results with the BEA in Fig. 3, we see that, with the exception of the $O^{+7}$ case, where the experimental error is quite large, our FBA calculation seems to be in somewhat closer agreement with experiment, especially for the cases of $O^{+4}$ and $O^{+3}$. Also, there does not seem to be a systematic relationship between the BEA and our results for the difference charge states.

In Fig. 4 we give the results of the FBA calculation along with experimental results of Dmitriev et. al.[24,25] for all the charge states of nitrogen in helium. The ionization cross sections were calculated in the same way that was described for the $O^{+i}$-He collisions, with the exception that for the electron loss from the $2s^2$ and $2p^{1,2,3}$ levels, $Z_p^f \neq Z_p^i$ (see eq. (8)). For these cases it was found that closer agreement with experiment was obtained if $Z_p^i$ was chosen, as usual, to be the screeened charge for a given level, but $Z_p^f$ was taken to be the asymptotic charge seen by the ionized electron. Thus to calculate the ionization of $N^{+i}$, we took $Z_p^f = (i + 1)$, for $i \leq 4$. For ionization of ions containing 2p electrons, we also recalculated the contribution from the 2s subshell with the additional screening from the outer electrons and the altered ionization potential. As in the O-He cases, the 1s subshell's contribution was not recalculated since it was much smaller than the 2s and 2p contributions.

From Fig. 4 we see that near the peak, the agreement of the calculated and experimental cross sections is quite good, especially for the $N^0$, $N^{+1}$, and $N^{+2}$ cases. For the $N^{+3}$ and $N^{+4}$ cases, the agreement at energies below the peak is rather poor; however, for energies near

the peak and higher, the agreement is quite satisfactory. In view of the accord of theory and experiment for $N^{+6}$ and $O^{+6}$, we found the discrepancy between our results and the data of ref. 24 in the case of $N^{+5}$ somewhat surprising; however, this seems to be resolved by the results of a subsequent, more refined experiment and analysis.[25] The triangles in Fig. 4 represent the "most probable" values of the total ionization cross section determined by Dmitriev et.al.[25] after considering the effect of metastable $(1s, 2s)^{1,3}S$ states remaining in the beam which reaches the collision chamber. The experimentally measured cross section, they find, is in general roughly a factor of two greater than the true cross section for ionization of helium like ions in their ground state. In the particular case of $N^{+5}$ this ratio appears to bring experiment and our FBA results into accord for energies near the peak of the cross section.

As mentioned above, in order to fit the data for $N^{+i}$, we had to take $Z_p^f = +(i+1)$ for $i \leq 4$. Fig. 5 illustrates the effect of using the asymptotic charge for $Z_p^f$ in the continuum state of $\mathcal{E}_{n,\ell}(k,q)$, eq. (8), by comparing with the case in which $Z_p^f \equiv Z_p^i$, where $Z_p^i$ is the effective charge appropriate to the initial bound state.[18] We have plotted total cross sections, $\sigma_{n,\ell}^T(Z_p^f, Z_p^i)$, for ionization from the $2p^2$ and $2s^2$ subshells of $N^{+1}$ and $N^{+3}$, respectively. The cross section $\sigma_{2p}^T(2.0, 3.80)$ approaches a value $\sim$ 40% greater than $\sigma_{2p}^T(3.80,3.80)$ at high energies, while $\sigma_{2s}^T(4.0,5.05)$ approaches a value $\sim$ 20% higher than $\sigma_{2s}^T(5.05,5.05)$ at high energies. Thus we see that, for $\sigma_{2p}^T(Z_p^f, Z_p^i)$, the difference between the two methods for choosing $Z_p^f$ is significantly larger than the experimental

error of $\sim$ 20%, with $\sigma_{2p}^{T}$ (2.0,3.80) giving results in excellent agreement with the data for $N^{+1}$ in Fig. 4.

## IV. Discussion

In order to summarize our results and to put them into perspective, we have adapted a figure from the review article by Madison and Merzbacher.[27] Fig. 6 is a schematic representation of the regions in velocity ($v \equiv V/(Z_p^i\ v_o)$) and charge ($Z_T/Z_p^i$) "space" in which the plane wave Born approximation (PWBA ≡ FBA), semi-classical approximation (SCA), and molecular orbital approach (MO) are expected to be appropriate. Although this representation was originally designed for completely stripped ions colliding inelastically with neutral atoms, and although the various boundaries are, of course, not as well defined as in the figure, we have plotted those regions in this space which correspond to our calculations. The low velocity end of each of the lines and areas labeled by projectile-target pairs corresponds to the lowest velocity at which there is qualitative agreement between our results and experiment. Thus for H-C and H-He systems, the FBA cross section for ionizing hydrogen agrees with the data at velocities which are consistent with the usual criteria for the validity of the FBA:

$$Z_T/Z_p^i << 1 \text{ and } Z_T/Z_p^i << v$$

For the $O^{+i}$ and $N^{+i}$ projectiles on helium, we find that the accord with experiment extends to velocities lower than expected and the extent to which the PWBA region of validity overlaps that of the MO and SCA is apparent. This comparison of calculated and experimental results is important in establishing the regions of validity of the FBA for application to collision systems of astrophysical interest for which

little or no data is available.

From a consideration of the results for the speci ic multi-electron projectile-target systems that we have calculated, we conclude that for the ionization of highly ionized heavy particles by light atoms, the FBA should give very reliable values of cross sections for velocities corresponding to the peak of the cross section and higher.

## ACKNOWLEGEMENTS

I would like to express my gratitude to Dr. K. Omidvar for many helpful discussions and especially for the use of his program for calculating the screened hydrogenic inelastic form factors. I am also grateful to Prof. F. W. Martin for a discussion of the oxygen-helium data. Finally I would like to thank A. Silver and E. Sullivan for their expert assistance in solving programming difficulties.

## REFERENCES


1. D. R. Bates and G. W. Griffing, Proc. Phys. Soc. A, 66, 961 (1953); ibid 68, 90 (1955); D. R. Bates and A. Williams, Proc. Phys. Soc., 70, 306 (1957).
2. For a review of the early work see D. R. Bates, in Atomic and Molecular Processes, edited by D. R. Bates (Academic Press, New York, N. Y., 1962), Ch. 14.
3. T. J. M. Boyd, B. L. Moiseiwitsch, and A. Stewart, Proc. Phys. Soc., 70, 110 (1957).
4. I. S. Dmitriev, Ya. M. Zhileĭkin, and V. S. Nikolaev, Zh. Eksp. Teor. Fiz. 49, 500 (1965) (Sov. Phys. J.E.T.P. 22, 352 (1966)).
5. V. S. Senashenko, V. S. Nikolaev, and I. S. Dmitriev, Zh. Eksp. Teor. Fiz. 54, 1203 (1968) (Sov. Phys. J.E.T.P. 27, 643 (1968)).
6. J. G. Lodge, J. Phys. B. 2, 322 (1969).
7. K. Omidvar and H. Lee Kyle, Phys. Rev. A 2, 408 (1970).
8. G. A. Victor, Phys. Rev. 184, 43 (1969).
9. A. N. Tripathi, K. C. Mathur, and S. K. Joshi, Phys. Rev. A 7, 109 (1973).
10. H. R. J. Walters, J. Phys. B, 8, L54 (1975).
11. H. Levy, II, Phys. Rev. 185, 7 (1969).
12. K. L. Bell, V. Dose, A. E. Kingston, J. Phys. B 2, 831 (1969).
13. J. S. Hansen, Phys. Rev. A 8, 822 (1973).
14. K. Omidvar, H. L. Kyle, and E. C. Sullivan, Phys. Rev. A 5, 1174 (1972).
15. Dž Belkić and R. Gayet, J. Phys. B. 9, L111 (1976).
16. H. L. Cox, Jr., and R. A. Bonham, J. Chem. Phys. 47, 2599 (1967).
17. D. T. Cromer, J. Chem. Phys. 50, 4857 (1969); D. T. Cromer and J. B. Mann, ibid. 47, 1892 (1967).

18. B. J. Block and L. B. Mendelsohn, Phys. Rev. A 12, 1197 (1975); also private communication.

19. C. Froese, J. Chem. Phys. 45, 1417 (1966); Univ. of British Columbia, Dept. of Mathematics, Technical Note (unpublished) 1966.

20. G. Burns, J. Chem. Phys. 41, 1521 (1964).

21. C. E. Moore, Atomic Energy Levels, Nat. Stand. Ref. Data Ser., National Bureau of Standards, Washington, D. C. 1971.

22. L. H. Toburen, M. Y. Nakai, and R. A. Langley, Phys. Rev. 171, 114 (1968).

23. P. M. Stier and C. F. Barnett, Phys. Rev. 103, 896 (1956).

24. J. R. Macdonald and F. W. Martin, Phys. Rev. A 4, 1965 (1971).

25. I. S. Dmitriev, V. S. Nikolaev, L. N. Fateeva, and Ya. A. Teplova, JETP 42, 16 (1962) (Sov. Phys. JETP 15, 11 (1962)).

26. I. S. Dmitriev, V. S. Nikolaev, Yu. A. Tashaev, and Ya. A. Teplova, Zh. Eksp. Teor. Fiz. 67, 2047 (1974) (Sov. Phys. JETP 40, 1017 (1975)); and V. S. Nikolaev, I. S. Dmitriev, Yu. A. Tashaev, Ya. A. Teplova, and Yu A. Fainberg, J. Phys. B 8, L58 (1975).

27. D. H. Madison and E. Merzbacher in Atomic Inner-Shell Processes, edited by B. Crasemann (Academic Press, N. Y., 1975), Vol. I, p. 59.

FIGURE CAPTIONS

Fig. 1. Projectile charge scaling of total ionization cross sections as a function of scaled relative velocity (eq. (8)) for hydrogen-like projectiles colliding with neutral He and C target atoms. (---) (lower scale) the $Z^4$ - scaled FBA result for electron loss by H, $O^{+7}$, and $Fe^{+25}$ projectiles of nuclear charge $Z \equiv Z_p$ in He. (——) (upper scale) the same processes in C. (a) data from ref. 22, and (b) from ref. 23.

Fig. 2. Total electron loss cross sections for $Fe^{+25}$ scaled as $(Z^4/Z_T^2)$ for various targets as a function of scaled relative velocity. Here $Z \equiv Z_p = 26$. (——) present FBA results for neutral target atoms of nuclear charge $Z_T$. (---) the BEA values from ref. 13, and (—·—) the FBAP result, both for bare nuclei as targets.

Fig. 3. Single electron loss cross sections for the ions $O^{+i}$ (i=3-7) in collision with neutral He as a function of laboratory energy (E/A) in MeV/nucleon. (——) and (—·—) present FBA results, (---) the BEA results for $He^{+2}$ targets. Data from (a) ref. 25, (b) ref. 24, (c) ref. 26, containing corrections for metastable states in the beam (see discussion of Fig. 4 in the text).

Fig. 4. Total ionization cross sections for the loss of one electron by $N^{+i}$ (i=0-6) in He, versus laboratory energy in MeV/nucleon. (— -) the present FBA results (a) data of ref. 25; (b) from ref. 26, after correction for metastables in the beam.

Fig. 5. Comparison of total ionization cross sections, $\sigma_{n,\ell}^{T}(Z_p^f, Z_p^i)$, resulting from choosing either $Z_p^f \equiv Z_p^i$ or $Z_p^f = (i+1)$ for the $(n,\ell)$ subshell of $N^{+i}$(i=1,3). a) $2s^2$ subshell of $N^{+3}$; (——··——)

$\sigma_{2s}{}^{T}(5.05, 5.05)$, (—- —) $\sigma_{2s}{}^{T}$ (4.0, 5.05). b) $2p^2$ subshell of $N^{+1}$; (---) $\sigma_{2p}{}^{T}(3.80, 3.80)$, (——) $\sigma_{2p}{}^{T}(2.0, 3.80)$.

Fig. 6. Schematic of the regions in charge and velocity space for which the molecular orbital approach (MO), the plane wave Born approximation (PWBA), and the semi-classical approximation (SCA) are expected to be applicable. The regions labeled by the projectile-target pairs $N^{+i}$-He, $O^{+i}$-He, H-C and H-He are for the results of the present work which are in accord with experiment.

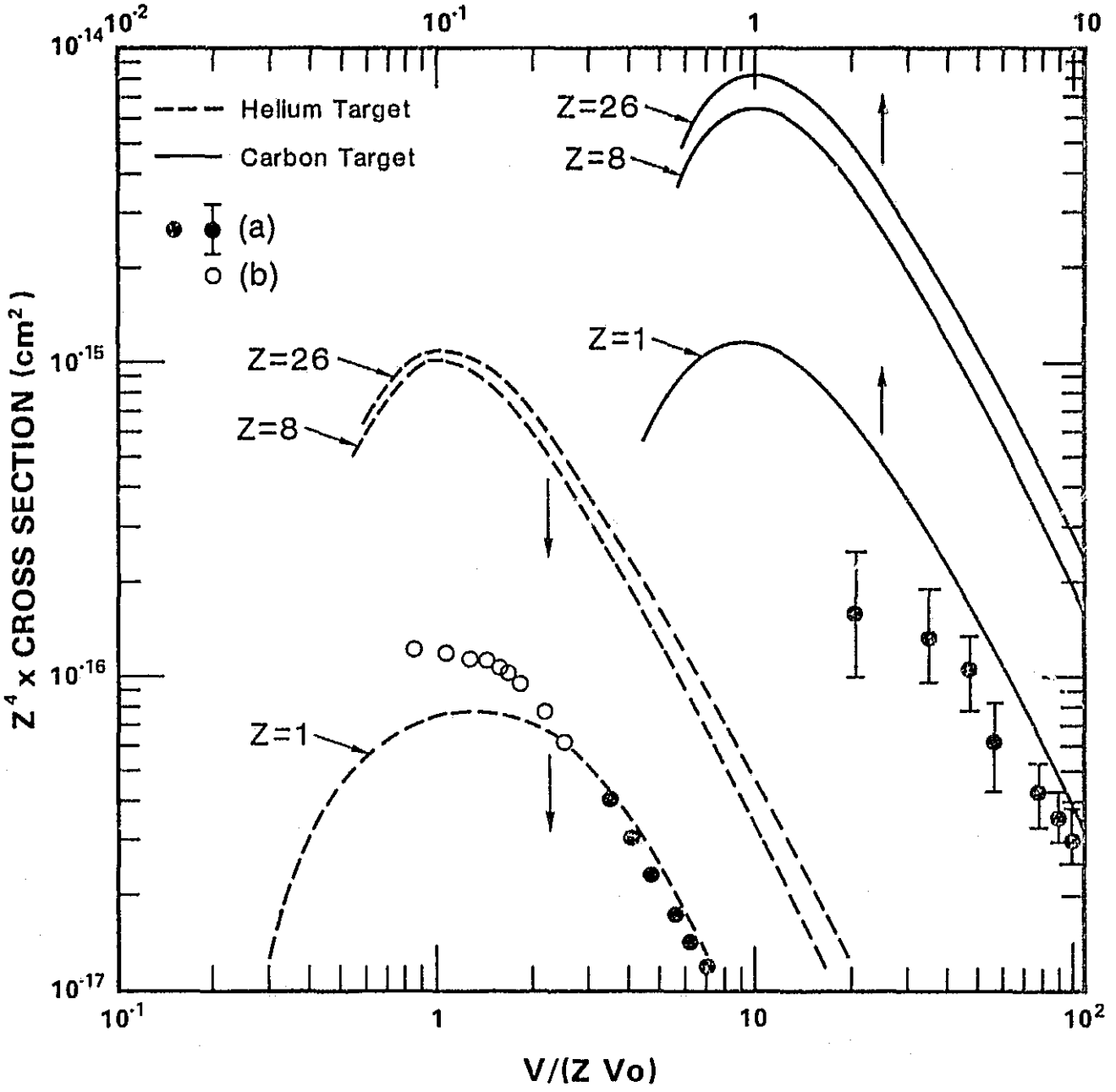
Hellum Target
Carbon Target
(a)
(b)
Z=26
Z=8
Z=1
Z=26
Z=8
Z=1
$Z^4$ x CROSS SECTION ($cm^2$)
V/(Z Vo)
$10^{-14}$
$10^{-15}$
$10^{-16}$
$10^{-17}$
$10^{-2}$
$10^{-1}$
1
10
$10^{-1}$
1
10
$10^{2}$

FIGURE 1

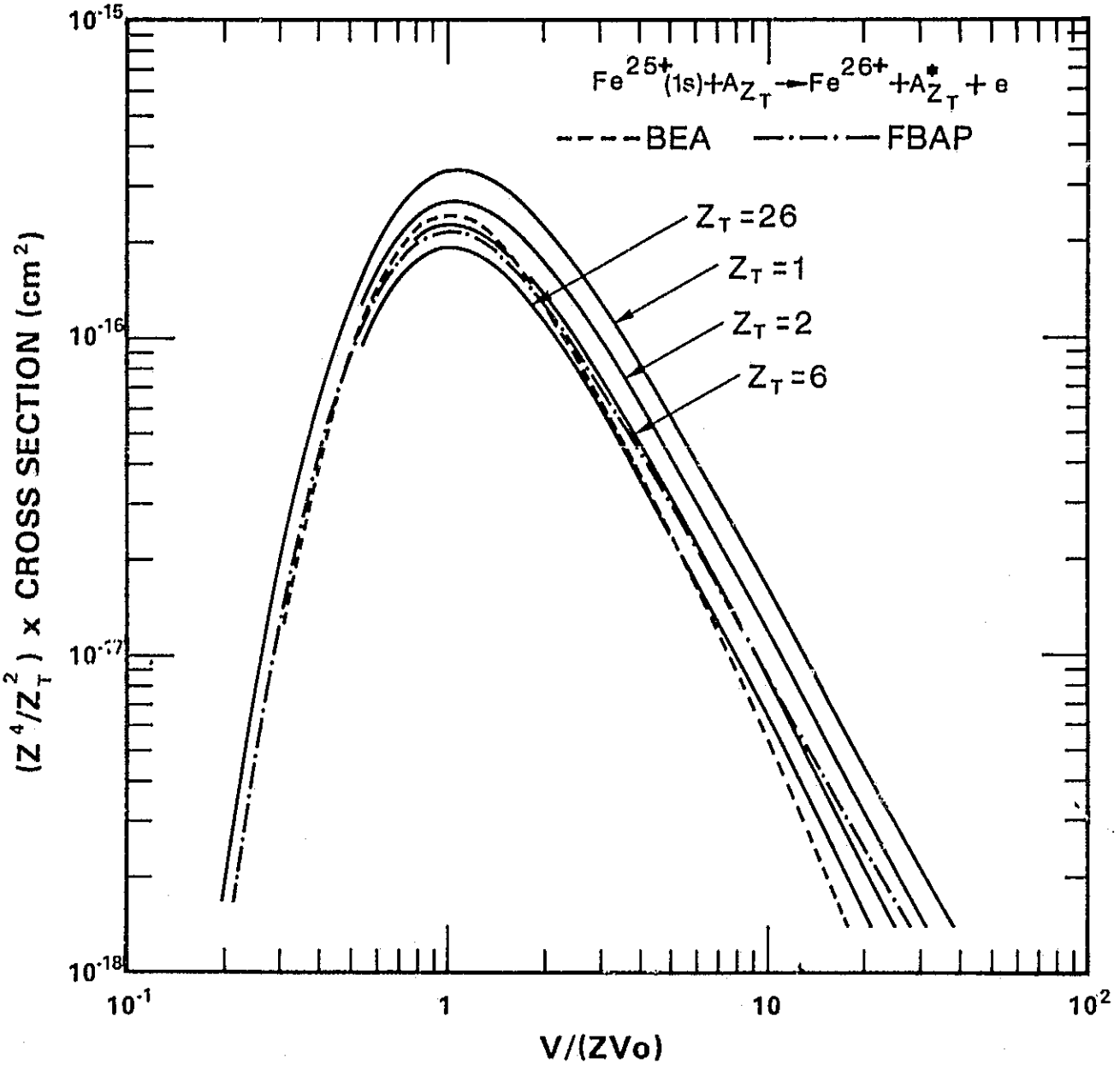
$Fe^{25+}(1s)+A_{Z_T} \rightarrow Fe^{26+}+A^*_{Z_T}+e$
BEA
FBAP
$Z_T=26$
$Z_T=1$
$Z_T=2$
$Z_T=6$
$10^{-15}$
$10^{-16}$
$10^{-17}$
$10^{-18}$
$(Z^4/Z_T^2) \times$ CROSS SECTION ($cm^2$)
$10^{-1}$
1
10
$10^2$
V/(ZVo)

FIGURE 2

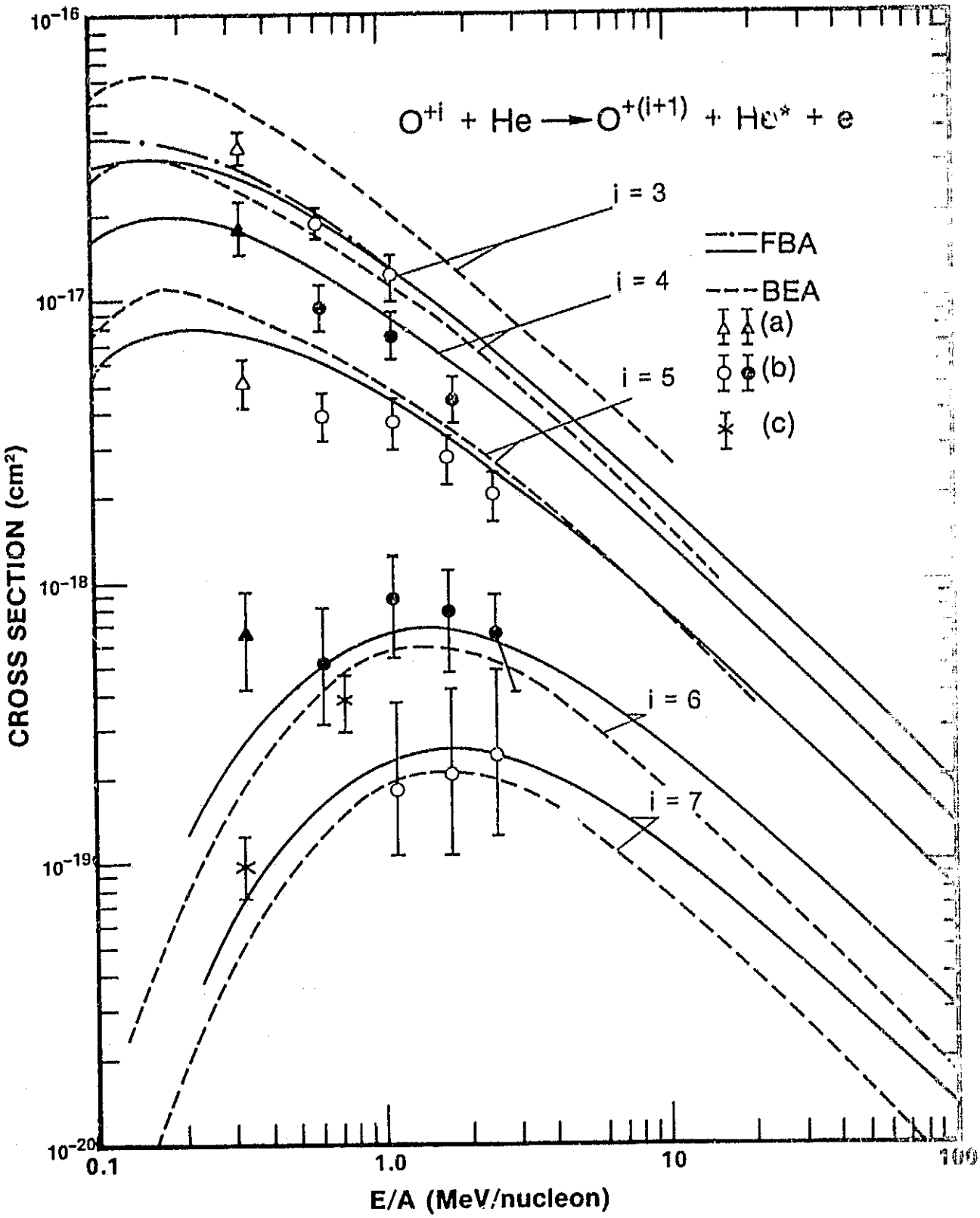
$O^{+i} + He \rightarrow O^{+(i+1)} + He^* + e$
i = 3
i = 4
i = 5
i = 6
i = 7
FBA
BEA
(a)
(b)
(c)
CROSS SECTION (cm²)
E/A (MeV/nucleon)
10⁻¹⁶
10⁻¹⁷
10⁻¹⁸
10⁻¹⁹
10⁻²⁰
0.1
1.0
10
100

FIGURE 3

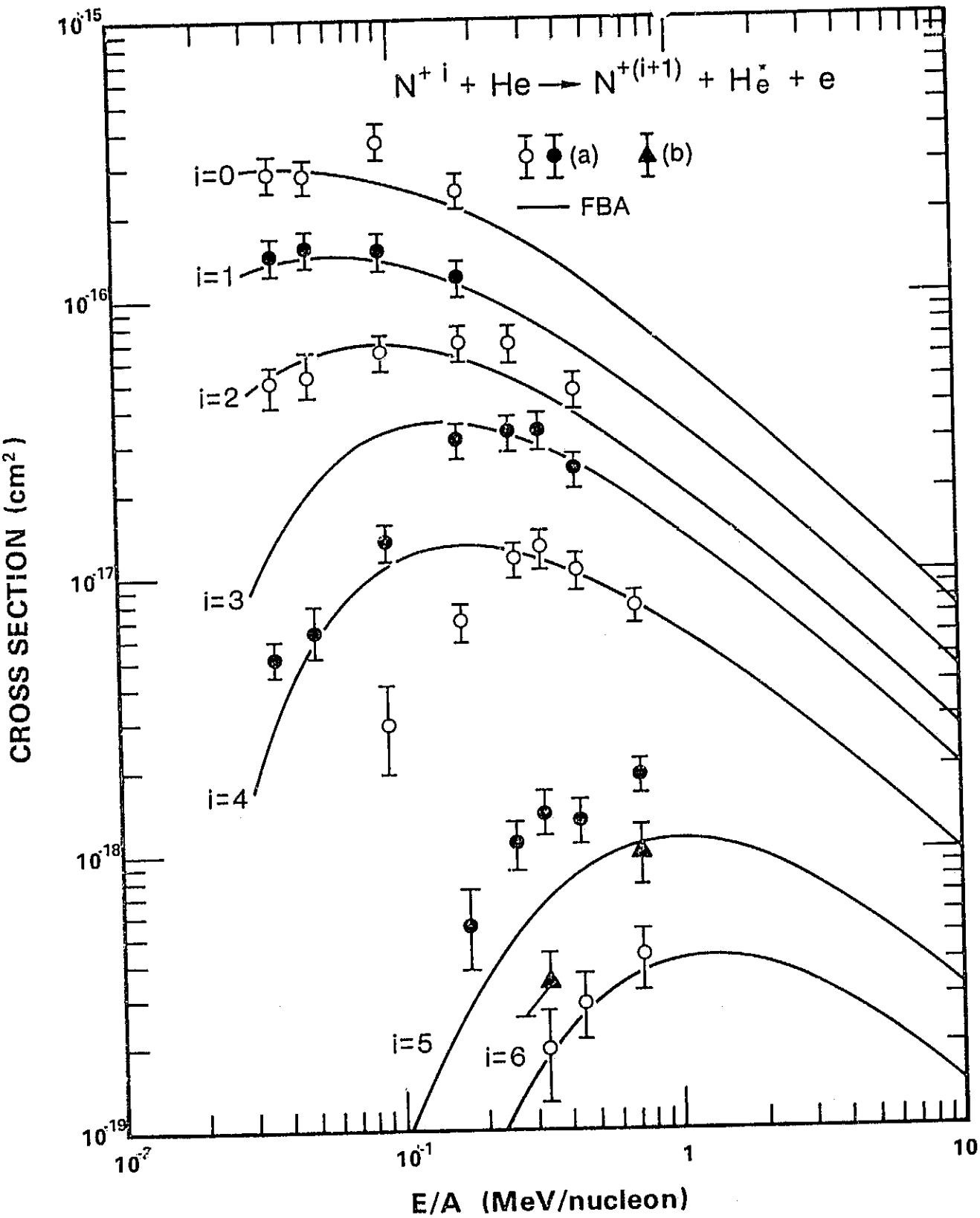
$N^{+i} + He \rightarrow N^{+(i+1)} + He^{*} + e$
(a)
(b)
FBA
i=0
i=1
i=2
i=3
i=4
i=5
i=6
CROSS SECTION ($cm^2$)
E/A (MeV/nucleon)
$10^{-15}$
$10^{-16}$
$10^{-17}$
$10^{-18}$
$10^{-19}$
$10^{-2}$
$10^{-1}$
1
10

FIGURE 4

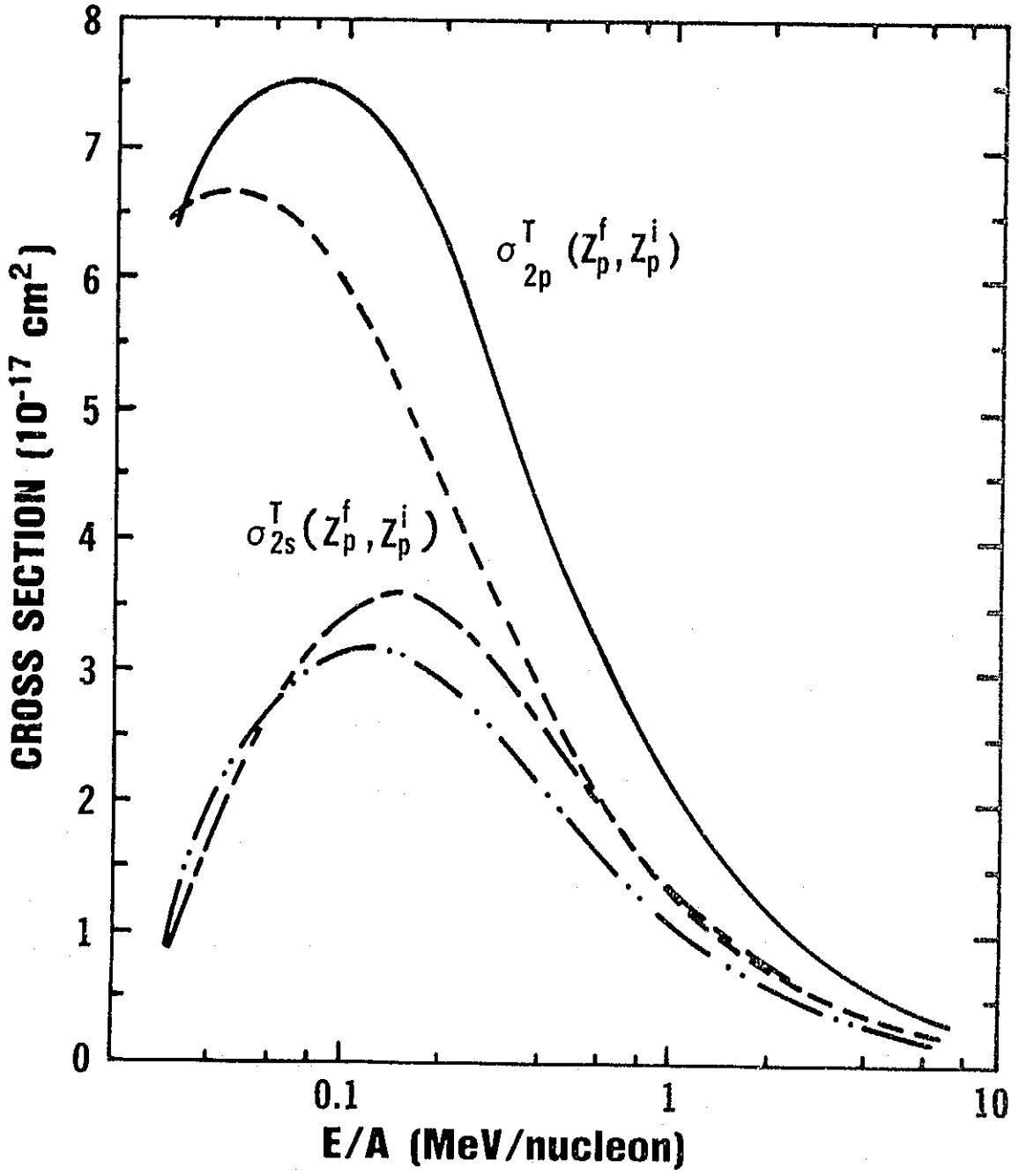
CROSS SECTION ($10^{-17}$ cm$^2$)
E/A (MeV/nucleon)
$\sigma^T_{2p}(Z^f_p, Z^i_p)$
$\sigma^T_{2s}(Z^f_p, Z^i_p)$
0
1
2
3
4
5
6
7
8
0.1
1
10

FIGURE 5

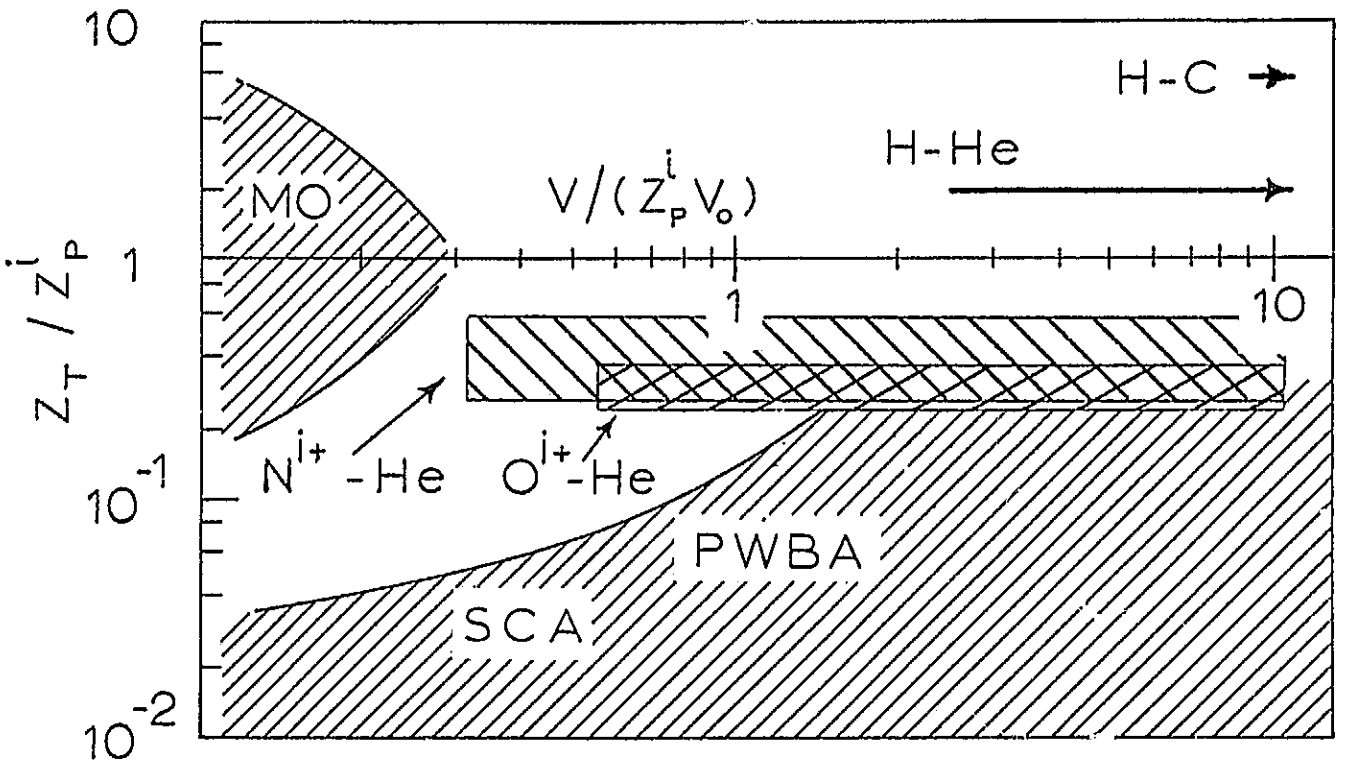


FIGURE 6